

Fast 3D velocity updates using the pre-stack exploding reflector model

Claudio Guerra and Biondo Biondi, Stanford University.*

ABSTRACT

In areas of complex geology, pre-stack depth migration is required not only for imaging purposes but also for velocity estimation. Migration velocity analysis based on wavefield extrapolation (Sava and Biondi, 2004; Shen and Symes, 2008) promises to produce more reliable results in those areas than its ray-based counterpart. However, due to the high computational cost, wavefield extrapolation methods are rarely used to estimate the migration velocity model in 3D projects (Fei et al., 2009), and therefore we face the challenge of decreasing the cost of migration velocity analysis by wavefield extrapolation while maintaining its robustness.

Usually, to decrease the cost of wavefield extrapolation data size is reduced by synthesizing plane waves (Liu et al., 2006) or by random-phase encoding (Romero et al., 2000). The prestack-exploding reflector model (PERM) (Biondi, 2006) introduces a new synthesized data, which significantly reduces data size. PERM data is computed by computing areal source and receiver wavefields using the exploding reflector concept, and starting from a pre-stack image migrated by wavefield extrapolation with an inaccurate velocity model. Guerra et al. (2009) show that further reduction can be achieved by randomly phase encoding the modeling experiments, significantly decreasing the cost of migration velocity analysis iterations. PERM wavefields can be propagated only in the region with velocity inaccuracies. Therefore, velocity updates can be performed in a target-oriented way, which contributes to an additional cost reduction of migration velocity analysis.

In 3D, reduction of the data size can be considerable if the initial image used to model PERM wavefields has only in-line subsurface offsets, as in the common-azimuth approximation. We show that 3D-PERM data size can be potentially up to two orders of magnitude smaller than 3D-plane wave data. The usefulness of PERM data to migration-velocity analysis with wavefield extrapolation is illustrated using a North Sea 3D dataset.

PRE-STACK-EXPLODING-REFLECTOR MODEL

The fundamental idea of PERM is to model data that describes the correct kinematics of an isolated SODCIG. When using Born modeling, since we do not know beforehand which shots contribute to forming the image at a point in the model space, we have to model several shots. Ideally, instead of performing many modeling experiments, we would like to synthesize a small amount of data with the condition that migration has

the same kinematics as the initial SODCIG. This can be achieved by extrapolating source and receiver wavefields starting from a pre-stack image computed with wave-extrapolation methods.

The modeling of PERM source D_P and receiver U_P wavefields can be carried out by any wavefield-continuation scheme. Here, we use the following one-way wave equations:

$$\begin{cases} \left(\frac{\partial}{\partial z} - i\sqrt{\omega^2 s_0^2(\mathbf{x}) - |\mathbf{k}|^2} \right) D_P(\mathbf{x}, \omega; \mathbf{x}_m) = I_D(\mathbf{x}_m, \mathbf{h}) \\ D_P(x, y, z = z_{\max}, \omega; \mathbf{x}_m) = 0 \end{cases}, \quad (1)$$

and

$$\begin{cases} \left(\frac{\partial}{\partial z} + i\sqrt{\omega^2 s_0^2(\mathbf{x}) - |\mathbf{k}|^2} \right) U_P(\mathbf{x}, \omega; \mathbf{x}_m) = I_U(\mathbf{x}_m, \mathbf{h}) \\ U_P(x, y, z = z_{\max}, \omega; \mathbf{x}_m) = 0 \end{cases}, \quad (2)$$

where $I_D(\mathbf{x}_m, \mathbf{h})$ and $I_U(\mathbf{x}_m, \mathbf{h})$ is the isolated SODCIG at the horizontal location \mathbf{x}_m for a single reflector, suitable for the initial conditions for the source and receiver wavefields, respectively. The subsurface-offset \mathbf{h} is parameterized as $\mathbf{h} = (h_x, h_y)$. The initial conditions are obtained by rotating the original unfocused SODCIGs according to the apparent geological dip of the reflector. By doing so, image-point dispersal is corrected such that the velocity information needed for migration velocity analysis is maintained.

To decrease the number of modeling experiments, linearity of wave propagation can be used to combine SODCIGs and inject them simultaneously into one single model experiment, using the same modeling equations as above with the initial conditions replaced by the combined SODCIGs. To obtain a crosstalk-free image after migrating PERM data, the SODCIGs combined in the same modeling experiment must be sufficiently separated such that unrelated wavefields do not correlate during migration. This distance determines the number of modeling experiments, which is twice the number of subsurface offsets.

PERM using a common-azimuth migrated image

In the way PERM is formulated, there is no restriction on the dimensionality of the pre-stack image used as the initial condition for the modeling, which means that if the original data have sufficient cross-line offsets as in the acquisition geometries with wide range of azimuths, the initial conditions are a five-dimensional hypercube on \mathbf{x} , h_x and h_y . In the case of narrow-azimuth acquisition, when using common-azimuth migration (CAM) we can assume zero cross-line offset and images are four-dimensional hypercubes in \mathbf{x} and h_x . Therefore, PERM data can be modeled by SODCIGs continuously sampled in the cross-line direction, which can yield one more order of magnitude of data reduction.

We modeled 3D-Born data on a 30° dipping reflector with 45° azimuth with respect to the acquisition direction. The velocity is the 1D function $v(z) = (1500 + 0.5z)$ m/s.

The Born data was input to CAM with a 5% slower velocity (Figure 1a). Source and receiver PERM wavefields were modeled with the same inaccurate velocity and using continuous sampling along the cross-line direction and sampling period of 48 in the in-line direction. The areal-shot migration of PERM data is shown in Figure 1b. The kinematics of the SODCIGs computed with PERM wavefields matches those of the SODCIGs computed with CAM.

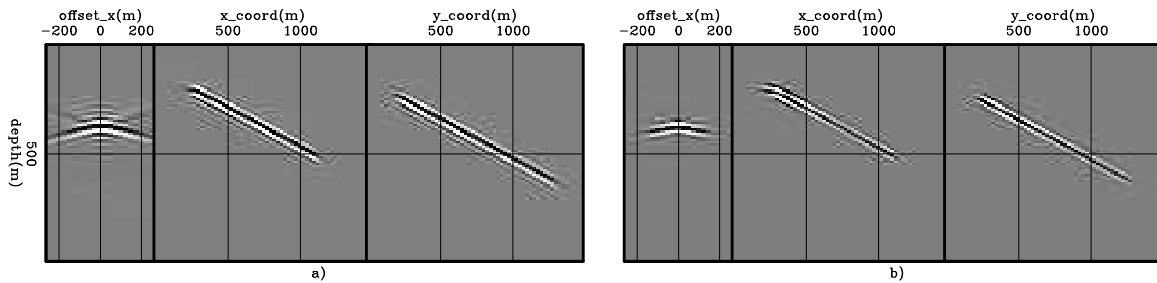


Figure 1: Migration results: a) CAM of the 3D-Born data, and b) areal-shot migration of PERM data. The panel on the left is the SODCIG at $(x = 750 \text{ m}, y = 600 \text{ m})$. The panel in the middle is the in-line at $y = 600 \text{ m}$ and the panel on the right is the cross-line at $x = 750 \text{ m}$.

EXAMPLE – 3D VELOCITY UPDATE

Migration velocity analysis by wavefield extrapolation using 3D PERM data was performed on a 3D real dataset from the North Sea with 3600 m maximum offset. This dataset was submitted to azimuth-moveout and imaged with CAM with an initial velocity sufficiently accurate up to the top of the chalk layer. From this reflector to deeper levels velocity (Figure 2a) is underestimated as revealed by reflectors curving up in angle-domain common-image gathers at the bottom of Figure 3a.

We synthesized 45 PERM wavefields for the base of chalk (**B** in Figure 3). The wavefields are collected at 600 m depth, which is close to the top of the target-zone. Therefore, during the migration velocity analysis wavefield propagation is performed between this depth level and 2800 m.

We computed velocity updates for the chalk layer in part of the 3D volume limited to the top of chalk, indicated by **T** in Figure 3. To optimize the velocity, we use a nonlinear conjugate gradient algorithm. The objective function we minimize is computed via differential-semblance optimization (DSO) (Symes and Carazzone, 1991; Shen and Symes, 2008). The updated velocity is constrained to be within bounds 50%-lower and 50%-higher the initial velocity. The optimized velocity model after 5 iterations is shown in Figure 2b for the in-line at 3760 m and cross-line at 3500 m. Notice that, as expected, the optimized velocity is higher than the initial velocity. CAM using the optimized velocity confirms the correctness of the velocity update, by showing more focused reflectors and flatter ADCIGs (Figure 3b) than that obtained

with the initial velocity. Residual moveout is still present as can be seen in the right-most ADCIGs. Close to this region, occurs a salt body which velocity was not taken into account by a salt flooding procedure.

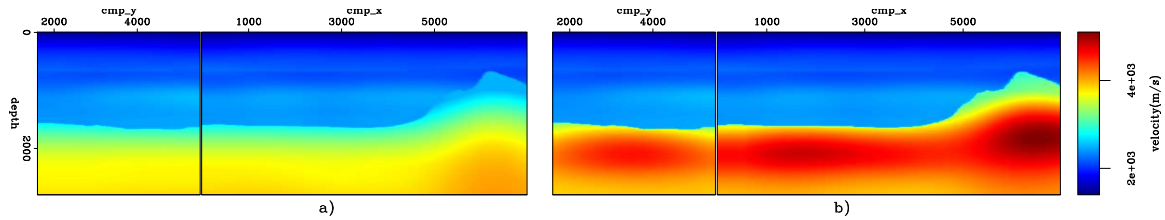


Figure 2: Velocity models. a) Initial velocity, and b) optimized velocity. Left panel: cross-line at 3500 m. Right panel: in-line at 3760 m.

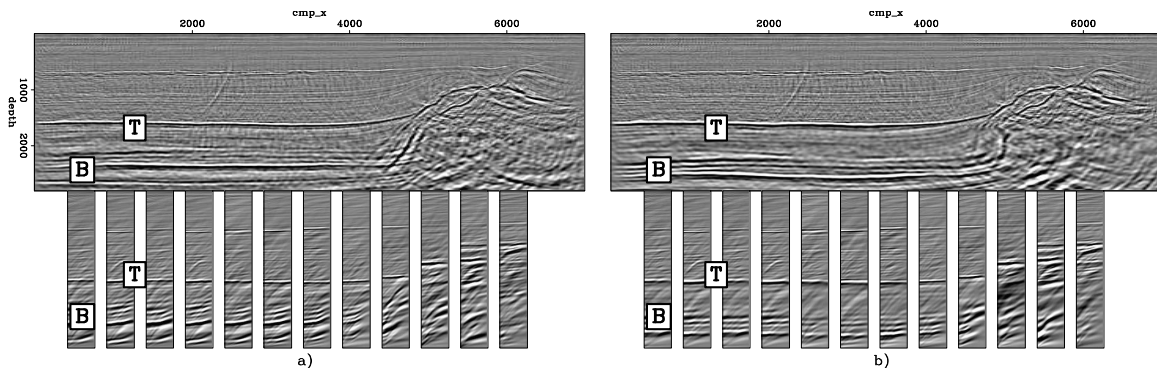


Figure 3: Angle-gathers. a) After CAM with the initial velocity, and b) after CAM with the optimized velocity. Top panel: zero-angle section. Bottom panel: ADCIGs from 0° to 40° selected at the same x position in the section above.

CONCLUSIONS

PERM synthesizes wavefields that provides migrated images with correct kinematics while decreasing data size. Data reduction is achieved by combining the modeling experiments and is controlled by the number of subsurface offsets that will be computed during areal-shot migration of PERM data. In 3D, PERM data size can be one order of magnitude smaller if cross-line subsurface-offsets are to be computed. Further data size reduction by one order of magnitude is achieved if the initial conditions are computed with common-azimuth migration.

In addition to the reduced data size, the ability PERM wavefields naturally have to be used in a target-oriented way greatly accelerates the definition of the velocity model. The 3D example with real data confirms the accuracy of the velocity solution achieved by migration velocity analysis by wavefield extrapolation using PERM wavefields.

ACKNOWLEDGMENTS

The authors thank TotalFinaElf for providing the data used in this paper and the sponsors of the Stanford Exploration Project for their financial support.

REFERENCES

- Biondi, B., 2006, Prestack exploding-reflectors modeling for migration velocity analysis: SEG Technical Program Expanded Abstracts, **25**, 3056–3060.
- Fei, W., P. Williamson, and A. Khoury, 2009, 3-D common-azimuth wave-equation migration velocity analysis: SEG Technical Program Expanded Abstracts, **28**, 2283–2287.
- Guerra, C., Y. Tang, and B. Biondi, 2009, Wave-equation tomography using image-space phase encoded data: SEG Technical Program Expanded Abstracts, **28**, 3964–3968.
- Liu, F., D. W. Hanson, N. D. Whitmore, R. S. Day, and R. H. Stolt, 2006, Toward a unified analysis for source plane-wave migration: Geophysics, **71**, 129–139.
- Romero, L., D. Ghiglia, C. Ober, and S. Morton, 2000, Phase encoding of shot records in prestack migration: Geophysics, **65**, 426–436.
- Sava, P. and B. Biondi, 2004, Wave-equation migration velocity analysis-I: Theory: Geophysical Prospecting, **52**, 593–606.
- Shen, P. and W. W. Symes, 2008, Automatic velocity analysis via shot profile migration: Geophysics, **73**, VE49–VE59.
- Symes, W. W. and J. J. Carazzone, 1991, Velocity inversion by differential semblance optimization: Geophysics, **56**, 654–663.